Int J Adv Manuf Technol (2016) 83:1671–1681
DOI 10.1007/s00170-015-7699-5

ORIGINAL ARTICLE

Laser beam micro-machining under water immersion

Abdulrehman M. Alahmari[1,2,4] · **Naveed Ahmed**[1,2,3,4] · **Saied Darwish**[1,2,4]

Received: 28 January 2015 / Accepted: 4 August 2015 / Published online: 18 August 2015

Abstract Underwater laser beam machining is considered as one of the alternative approaches to minimize the undesired impacts of dry laser beam machining (LBM) such as coarse machining kerf, high re-deposition of melt debris, and thermal damages. The underwater laser beam machining is equally suited for the fabrication of micro-features like 3D cavities, micro-holes, and micro-channels. In most of the literature studies, the water in dynamic mode (flowing with certain flow rate) is generally used to reduce the melt re-deposition and to improve the machining kerf and surface roughness. This study presents the use of water in static mode (still water with zero flow rate) rather dynamic mode, for the fabrication of micro-channels in nickel-based superalloy (Inconel 718). Instead of reducing the melt re-deposition, static water allowed to deposit more debris within the machining zone. This re-deposition is used to participate in micro-channel formation. After every initial passing scan, the re-deposited melt debris are piled up at the middle region of main channel that disturbs the beam focus at middle region. Due to focus disturbance, the piled up debris gets removed by partial melting of the central region and base metal remains unaffected due to partial heating. The main channel finally divided into two sub-channels. Geometrical characteristics (width, depth, and taper angle) were considered as the process responses in order to study the effects of laser power, pulse repetition rate, and laser scan speed. The results revealed that among other parameters, laser scan speed mainly influenced the geometrical characteristics of micro-channels.

Keywords Laser beam machining · Micro-channel · Inconel 718 · Water film · Scan speed

✉ Naveed Ahmed
anaveed@ksu.edu.sa

Abdulrehman M. Alahmari
alahmari@ksu.edu.sa

Saied Darwish
darwish@ksu.edu.sa

[1] Industrial Engineering Department, King Saud University, Riyadh, Saudi Arabia

[2] Advanced Manufacturing Institute, King Saud University, Riyadh, Saudi Arabia

[3] Department of Industrial and Manufacturing Engineering, University of Engineering and Technology, Lahore, Pakistan

[4] Princess Fatima Alnijiris's Research Chair for Advanced Manufacturing Technology (FARCAMT), King Saud University, Riyadh, Saudi Arabia

1 Introduction

Laser beam machining (LBM) is conventionally performed under air. In recent days, the process is performed under wet atmospheric conditions in place of air. These wet conditions include the use of ethanol, methanol, acetone, and water, etc. [1]. The purpose of liquid is generally to reduce the thermal damages caused by the laser ablation under air atmosphere. Underwater laser processing provides a solution to the majority of the problems of laser machining in air and other gasses, especially heat-affected zone (HAZ) which can substantially be avoided due to the additional cooling action of water layer/jet [2]. In literature, significant research is available, attempting underwater laser processing in order to alleviate the defects around the laser cut grooves and holes in both metals [3] and non-metals [4]. The research shows that the water environment is a great candidate for material removal by laser, especially where coarse removal is required [5]. Ablated surface attributes, geometrical aspects (width, depth, and aspect ratio), melt re-deposition, and HAZ are generally evaluated and compared with laser ablation in air. Nevertheless, the investigations of the ablation rate are a highly

common attribute. The results are entirely based on the material and the laser-water parameter settings, mainly laser fluence, pulse numbers, repetition rate, spot diameter, and water layer thickness. That is why the results are not consistent in literature, especially for ablation rate. For example, the study documented in [6] shows that in liquids, the temperature of confined plasma remains higher than in air; thus, the liquid prevents the plasma expansion [7] that enriches the laser radiation energy [8] and consequently improves machining rate [9]. The projected shock pressure in water and air environment are ~3 and ~95 MPa, which means high pressure by water produces shock waves that lower the viscosity of molten material. Thus, efficient material removal and ejection rate can be achieved [10]. The authors of [11] stated that the micro-bubbles carry more efficiently the melt debris away that speeds up the ablation process. On the opposite side, many researchers reported low ablation in underwater conditions. For instance, the research conducted by [12] concluded that the liquid layer thickness absorbs the high proportion of laser energy and attenuates the energy transmitted to target surface. This lowers the ablation efficiency. The investigators of [13] proved that the liquid's absorption coefficient that depends on laser wavelength creates the difference in ablation rate. Low absorption coefficient enhances the ablation performance and vice versa [6]. In the study documented in [12], the fabrication of holes in Si is presented. The results revealed that the ablation depth is mainly dependent on the number of pulses and the fluence level. They reported threshold fluence of 2 J/cm^2 underwater processing and 1.7 J/cm^2 in air. It means that the machining depth is low by underwater laser ablation compared to dry ablation.

Laser ablation in the presence of water is equally suited to mill 3D geometries in almost all kinds of materials. Similar to other advantages and applications, it is greatly applied to achieve high geometrical precisions with good surface quality. The experiments in [8] indicate that the precision and quality of machined cavity in SiC ceramics are high by underwater laser machining compared to machining in air. The laser machining of magnetic materials (NdFeB and ferrite) under water found to give much higher surface finish and elimination of debris than in air [14]. 3D cavities and micro-holes have also been achieved by femtosecond laser ablation in the water ambient by [15] where the researchers introduced distilled water from the rear surface of the glass substrate. They claimed that the same method can be employed to produce micro-channels on transparent materials. Crater and nanostructures in air and water are experienced by [10] on brass and aluminum. Under thin layer of water, the laser machining of micro-grooves in Ti6Al4V can be seen in [16], where the reporting team evaluated the cut quality and crack formation around and beneath the groove. They also stated that the presence of flowing water significantly disturbs the laser beam energy prior to reaching the target surface. Therefore, thinner water film increases the machining efficiency.

In most of the studies related to underwater laser machining, as described above, the researchers used the distilled water in dynamic mode with certain flow rate. The flow rate generally ranges within 10–30 ml/s [17]. The main purpose of flowing water in underwater laser ablation is to facilitate the melt debris so that a clean profile can be achieved. It is reported that the flowing water in LBM results a negligible amount of melt's re-deposition and lowers the ablation rate [18]. The fabrication of micro-channels in polymethyl methacrylate (PMMA) using Nd:YAG laser passing through flowing stream of water can be seen in [19] where the authors stated that underwater laser processing with flowing water results into less re-deposition around the micro-channels, and consequently, cleaner and finer structure can be acquired. Similar remarks are concluded by the investigators of [20] after laser processing of aluminum target under dry and water atmospheric conditions. They also used the concept of flowing water in order to minimize the re-deposition of melt debris.

It is worth noting that the machining of Inconel 718 to fabricate 3D geometries such as micro-grooves and micro-channels via LBM in air or in water has not been found in the open literature. In recent days, many attempts have been made to improve the machinability of these materials especially Inconel 718 more effectively via non-conventional processes (such as electric discharge machining (EDM) [21] and [22], abrasive waterjet machining (AWJM) [23], electrochemical machining (ECM) [24, 25], etc.) or by the use of external energy assisting the conventional machining (like laser-assisted machining (LAM) [26–28], vibration-assisted machining (VAM) [29], plasma-enhanced machining (PEM) [30], etc.). It should be noted that the use of laser energy is mainly utilized either for assisting the conventional machining process [26–28] or solely to modify the surface properties [31, 32]. To the authors' best knowledge and as per open available literature, no other study has been found discussing the machining of Inconel 718 via laser beam machining in air or in water environment.

The present study has been conducted to fabricate the micro-channels in Inconel 718 through Nd:YAG laser beam machining. The machining was performed under a constant layer of water at static mode rather than the water flowing inside the machining zone. Instead of minimizing the re-deposition of melt debris, the objective was to utilize the melt debris in the form of re-deposition mainly at the central region of the channel. These piled up debris mainly disturb the beam focus for each forthcoming fresh layer and the beam focus penetrates inside the surface of central location. At this central location, the base metal just heated up rather melting, while the partial melting occurs just at the surface leading to remove the deposited debris. In this way, the main channel was divided into two sub-channels. The width, depth, and taper angle of micro-channels were set as process responses to speculate the effects of process parameters.

2 Experimental setup

This study was carried out to understand the effects of laser process parameters on the ablation performance under fluidic environment during the development of micro-channels. For this purpose, a CNC Q-switched Nd:YAG laser system of *Deckel Maho* (Lasertec 40 manufactured by *DMG Mori Sieki*) [33] was utilized. From the YAG rod, the system produces pulsed laser beam of 1064 nm wavelength with pulse duration of 10 μs that follows the Gaussian mode. The average power of 30 W was available to utilize at any level. Instead of utilizing the full laser power, different levels of power were used. Depending upon the aperture size, the system can generate beam with spot diameter of 30 and 80 μm. However, in our present series of experiments, 30-μm spot size was selected due to its high energy intensity. The high energy intensity is generally considered as more suitable for milling purposes. The magnitudes of average laser intensities generated by both of these spot diameters are 42.441 and 5.968 kW/mm^2, respectively. Pulsed power is the accumulation of laser pulsed energy over a relatively long period of time and releasing it very rapidly. Thus, the instantaneous power increases, termed as peak pulse power (PPP). Likewise, the PPP of 3–10 MW/s can be acquired based upon the pulse duration and average laser power. These quantitative values were not measured during this study; however, these can be obtained from the Eqs. (1) and (2) [34].

$$I = \frac{P}{\pi\left({}^{d}/_{2}\right)^{2}} \tag{1}$$

$$\mathrm{PPP} = \frac{P}{\tau} \tag{2}$$

where P is the power (30–100 W), d is the beam spot diameter (30–80 μm), and τ is the pulse duration (10 μs).

The system is equipped with a CNC-controlled worktable movable in three transverse directions (X, Y, and Z) and a galvanometer head containing the optical lense(s) assembly. The laser or galvanometer head is capable to focus the laser spot on the targeted substrate. For major travels (>65 mm), the table executes linear motion, whereas for minor movements (≤65 mm), the galvanometer adjusts the lenses' positions according to the focal distance and depth of cut.

To investigate the effects of laser parameters under fluidic environment, distilled water of pH 6.89 (measured by HI 98129 pH meter manufactured by *Hanna Instruments*) [35] was used. The objective was to keep the setup as simple as possible in practical viewpoint. Therefore, the substrate was placed in cylindrical container of PMMA in such a way that the substrate can fully submerge in water. The schematic configuration shown in Fig. 1 depicts the arrangement of work sample relative to laser system. Water film thickness from the workpiece top surface was varied from 0.5 to 2 mm by an increment of 0.5 mm. In case of 0.5-mm film thickness, the substrate surface was not fully submerged in water, especially when the laser beam started to ablate the surface. On the other hand, the attenuation of laser energy depends on water film thickness. So, compared to 1-mm water film thickness, 2-mm film thickness attenuated more laser energy. Thereafter, the average water film thickness was fixed at 1 mm during the final series of experimental runs. This water film thickness above workpiece was obtained from the total volume law using Eqs. (3), (4), and (5).

$$V_{\mathrm{w}} = V_{\mathrm{wc}} - V_{\mathrm{s}} \tag{3}$$

$$V_{\mathrm{wl}} = A_{\mathrm{wc}} \times t_{\mathrm{w}} \tag{4}$$

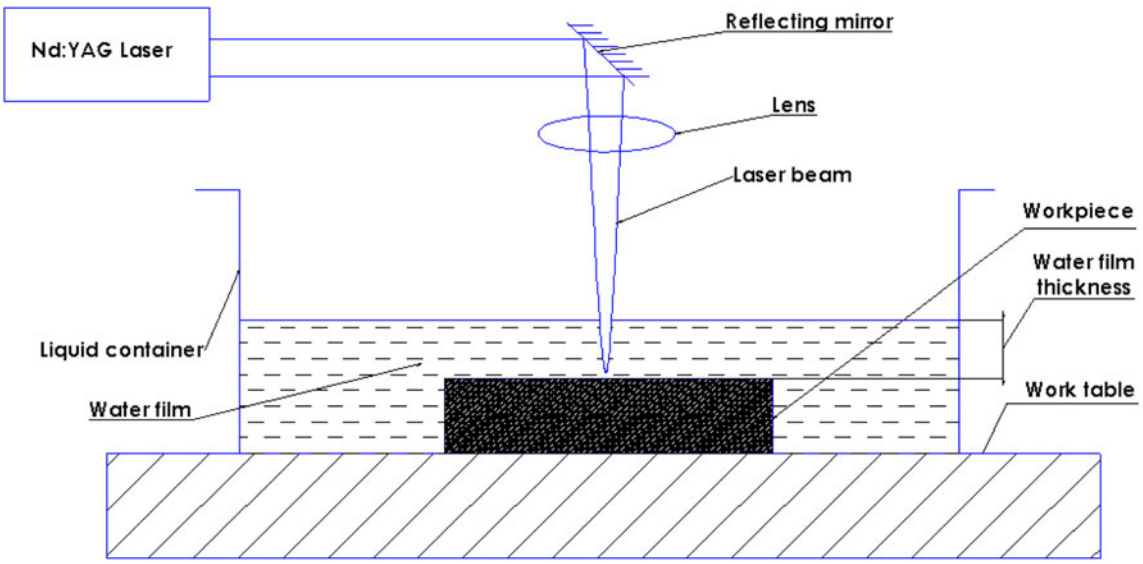

Fig. 1 Schematic configuration of underwater laser setup

$$V_{\text{total}} = V_{\text{w}} + V_{\text{wl}} \quad (5)$$

where

V_{w} Volume of water at the level of substrate
V_{wc} Volume of water container at substrate height
V_{s} Volume of substrate
V_{wl} Volume of water with average film thickness t_{w}
A_{wc} Area of water container base
t_{w} Average water film thickness
V_{total} Total volume of water required

Square cross-sectional bars (6×6×25 mm) of Inconel 718 (supplied by Magellan Metals, USA) [36] was used to ablate the microsized channels. The chemical composition of Inconel 718 is supplied in Table 1. The specimen was initially grinded and flattened to ensure the flat surface for uniform focal distance to irradiated laser beam. The micro-channel of size 100× 100 μm was designed to machine in nickel-based superalloy (Inconel 718) under fluidic environment. The computer-aided design (CAD) of each channel was developed on the machine's supplied design software (LPSWin) [33]. After the geometrical CAD development, the LPSWin generates a coded programmed file and transfers to the machining unit. It is essential to have a match of parameters of the programming file and the machine parameters. Important parameters include laser track displacement, layer thickness of material removal per laser scan, and scan direction. For the current study, these parameters were fixed at 10 μm, 2 μm, and random direction scan, respectively. The channel design was planned in such a way that each successive channel was milled at a distance of 1 mm away from the proceeding channel (3D view shown in Fig. 2). It allowed to keep the incoming channel free from the ablation effects of proceeding channel. The observations showed that the whole geometry of each channel was totally unaffected from its other neighboring channel's influence.

Table 1 Chemical composition of as received Inconel 718 [36]

Element	Percent
C	.03
Mn	.08
Fe	18.36
S	.001
Si	.07
Cu	.12
Ni	53.54
Cr	18.31
Al	.57
Ti	.88
Co	.20
Mo	2.86
Ta	.004
B	.002
Nb	4.86
P	.008

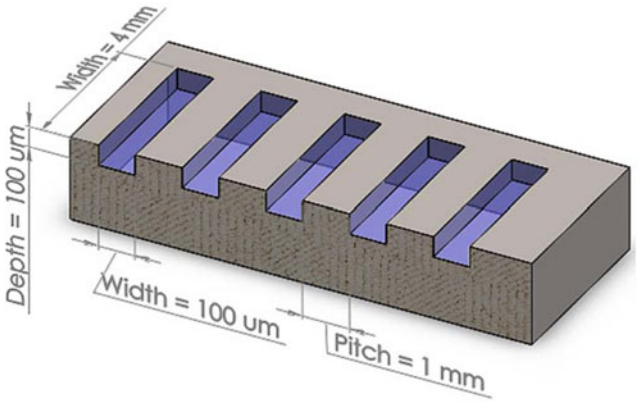

Fig. 2 A 3D view of designed channels (dimensions are not to scale)

The objective of this research was to determine the process potential for the fabrication of micro-channels under water with most appropriate parametric settings. The channel's width and depth of 100 μm each was experienced as the appropriate dimension to be suitably machined. This size selection was the outcome of pilot study in which the width and depth was kept at 50 μm each where the removal of ablated melt debris offers high resistance with very coarse machining results. The length of each channel was kept to 4 mm of length so that after cross-sectioning the samples, the significant amount of length could be available for microscopic and dimensional analysis.

There are various studies available in literature regarding underwater laser machining. Some of these studies are described in the Section 1. With the help of literature findings and the machine's suggested procedure, the initial screening of variables was performed by intensive set of experiments. A sequential procedure was followed to find out the list of fixed factors and the set of significant variable factors influencing the set responses. This procedure comprises of selection of level and range of a factor by response analysis. Initially, a selection criterion was established. Then, the response analysis was performed to evaluate the factor range whether it significantly or insignificantly affects the response. Similarly, the screening of parameters was conducted using regression analysis. Thus, the three variable factors were identified as the significant factor affecting the set responses. The list of fixed factors is presented in Table 2 depicting the available range, selected value, and selection criteria of each factor. In a similar manner, Table 3 shows the list of variable factors, range, and their selection criteria. Three numbers of laser-based predictors (naming: laser power, P; repetition rate, f; and scan speed, v) have been preferred to evaluate three numbers of dimensional-based responses (naming: width, W; depth, Z; and taper angle, θ). Each predictor has been tested against each response with various levels ranging from low to high, although the levels were not uniformly distributed but with

Table 2 List of fixed parameters with available range and selected values

Factor name	Available range	Selected value	Reasoning
Laser type (L)	Q-Switched Nd:YAG	–	–
Wavelength (λ)	1064 nm	–	–
Pulse duration	10 μs	–	–
Beam diameter (□)	▪30 μm ▪80 μm	30 μm	Narrower is the beam radius, less is the spot size. Low spot size creates more energy to ablation
Scan direction (X)	▪ Uniform horizontal ▪ Uniform vertical ▪ Mixed/random	Mixed / Random	Uniform direction creates scan impressions, while random scan is more suitable for good quality
Layer thickness (LT)	2–6 μm	2 μm	Small is the depth of cut, uniform is the ablation rate
Number of passes (N)	As many as we can	100	Required for channel depth against 2 μm LT
Scanning track displacement (D)	2–20 μm	10 μm	Superimposing of laser tracks is more for less value of D which is not required
Focal point (d)	≥0	0	$d>0$ causes low ablation or surface heating instead of material removal

various points. For example, laser power was switched from 27.72 to 28.92 by an average increment of 0.5 W. Likewise, repetition rate from 30 to 40 kHz with sequential difference of 5 kHz. Similarly, scan speed from very low speed of 10 mm/s to high speed of 400 mm/s was established. All the experiments were carried out by successive analytical results from one session to the other. The average water film thickness from workpiece top surface was varied from 0.5 to 2 mm with an increment of 0.5 mm. In case of 0.5 mm film thickness, the substrate surface was not fully submerged in water, especially when the laser irradiations initiate the ablation on substrate surface. Therefore, the water film thickness was kept constant and maintained at an average of 1 mm during the final series of experimental runs.

3 Machining mechanism

During underwater laser beam machining, the real machining is caused by laser energy. The function of water is to restrict the realization of undesired defects such as HAZ, spatter, melt re-deposition, and cracks, etc. However, the occurrence of these defects still exists in the presence of water but at low level. The material removal mainly depends on laser parameters (especially spot diameter, laser intensity or laser power, and scan speed) and the fluid dynamics (particularly fluid film thickness above work surface). The water film thickness above workpiece surface plays an important role in the ablation mechanism. It mainly decides the machined depth and kerf width [41]. The thick water layer carries away the debris more efficiently but also reduces the ablation rate. When the laser beam travels through the thick liquid film, the pulse shape does not remain uniform and/or consistent. At the laser-work interface, the formation of milky suspension composed of liquid and bubbles and melt debris is formed that confines the plasma above target material. It scatters the laser light along with a distortion of the laser pulse, and consequently, the energy, which needs to ablate the material, severely affects. High proportion of energy is absorbed by thick water film and thus attenuates the amount of energy to be absorbed by workpiece material leading to less ablation efficiency [12]. This attenuation of energy can be linked with Beer-Lambert's law of energy absorption. Relating this law to laser intensity transmitted through thin layer of water is expected to be low as

Table 3 List of variable parameters with their range and selection criteria

Factor name	Range	Selection criteria	Reference
Laser intensity (I)	90–98 %	Pilot experiments Lasertec 40 manufacturer's catalogue Literature results	[3, 37]
Pulse repetition rate (f)	30–40 kHz	Lasertec 40 manufacturer's catalogue Literature studies	[38–40]
Scan speed (v)	10–400 mm/s	Pilot experiments Literature results	[38–43]
Fluid film thickness (t)	1–2 mm	Pilot experiments Literature conclusions	[41, 44–46]

compared to the intensity transmitted when the water film thickness is high. The actual laser beam intensity transmitted to substrate after passing water film thickness of t_w can be calculated using Eq. (6).

$$I = I_o \exp(-\alpha_w t_w) \tag{6}$$

where

I Actual transmitted intensity
I_o Intensity above water film
α_w Absorption coefficient of water
t_w Water film thickness above substrate

As the absorption coefficient depends upon the wavelength of incident light, so the corresponding value of α_w is 0.135 cm^{-1} for laser beam of wavelength 1064 nm [47]. The water splashing within the closed premises of laser beam is a common phenomenon that generates the non-uniformity of water layer thickness [17]. Similarly, the formation and diffusion of cavitation bubbles is another physical phenomenon of underwater laser machining that disturbs the uniform water film thickness in static mode. Therefore, an approximation in the calculation of transmitted laser intensity has to be necessarily considered.

4 Results and discussions

In order to speculate the actual ablation performance, none of the sample was post processed. As per requirement of the geometrical analysis, the samples were just cross-sectioned by CNC wire-cut electric discharge machine (*ecocut* supplied by E*lectronica*) [48]. Each channel's configuration was very carefully observed and measured from the microphotographs obtained from *JEOL's* scanning electron microscope (SEM). The experimental runs are divided into two categories: fabrication of micro-channels under (1) low scan speeds, 10–60 mm/s and (2) high scan speeds, 70–400 mm/s. The results are also classified into two categories.

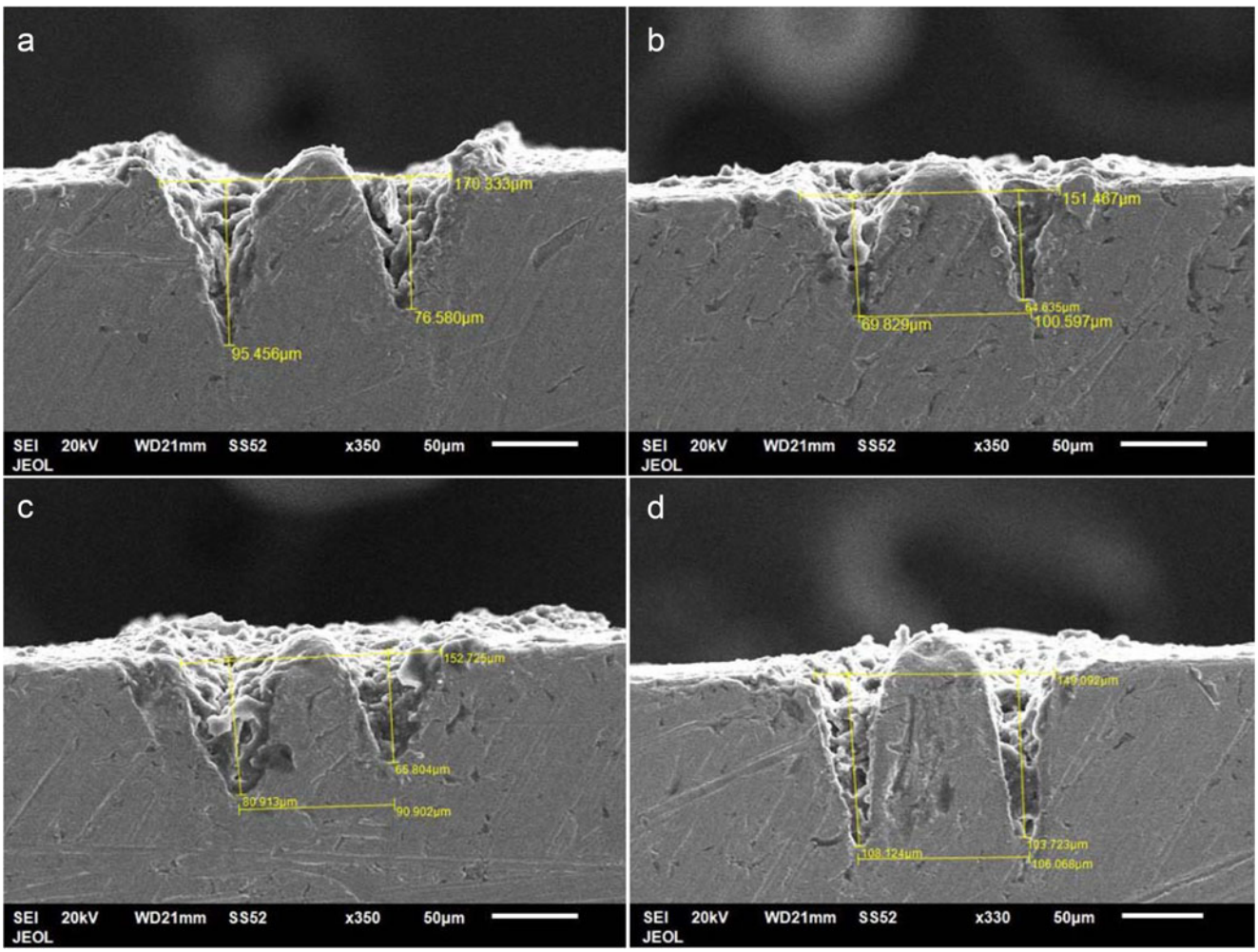

Fig. 3 Micro-channels fabricated under water at **a** t=1 mm, P=28.2 W, f=35 kHz, v=15 mm/s; **b** t=1 mm, I=28.2 W, f=35 kHz, v=30 mm/s; **c** t=1 mm, I=28.2 W, f=35 kHz, v=40 mm/s; and **d** t=1 mm, I=28.2 W, f=35 kHz, v=50 mm/s

4.1 Micro-channels under low scan speeds

Under this category of experimentation, micro-channels of cross-sectional size 100×100 μm were machined to see the process outcomes, in terms of machined geometries under low scan speeds. Referring to the previous studies of [38, 41, 42], the suggested scan speed for underwater laser ablation should be generally below 100 mm/s. Therefore, in this set of experimental runs, scan speed at low levels ranging from 10 to 60 mm/s with a successive increment of 5 mm/s was the only variable factor under investigation. The laser power, pulse repetition rate, and average water film thickness were maintained at constant values of 28.2 W, 35 kHz, and 1 mm, respectively. The settings of laser power and repetition rate were obtained from trial runs and the procedural recommendations of the utilized Lasertec 40 system. The SEM analysis of microphotographs (presented in Fig. 3) reveals the fact that the LBM under water environment produces set of two sub-channels when machining single channel. The formation of two sub-channels instead of one is mainly the result of re-deposition of melt debris and beam focus disturbance. Detailed explanation is discussed ahead.

Although the channel appearance is very coarse, but it is vigilant to see that deep channels can be obtained using low scan speed of laser tracks. The coarse nature of micro-channels in this low scan speed regimes is expectedly due to long interaction time of laser pulse with the ablation surface. Long interaction time allows the laser irradiations to melt the material in excess that leads to insufficient ejection of molten debris. As there is no additional supply of material ejection provided, the only medium to flush away the molten debris is the high pressure water plume observed in situ around the channel periphery. This inefficient material flushing causes the majority of debris to re-solidify on the ablated region and the around the channel. At the initial few ablated layers, the water plume pressure flushes more efficiently and re-solidification is less. But, when the ablation layers go deeper and deeper towards channel depth, the molten debris need to travel more vertical distance to reach at the channel top level and flush away from the channel boundaries. Therefore, the flushing phenomenon loses its efficiency at the deeper sections. Thus, in this way, the re-deposition of debris occurs more soundly. With respect to top surface, the re-deposition occurs in two outward V-shaped directions. Partial ejection and re-deposition is towards channel's outer edge, while the remaining debris stay on the unaffected region (region without machining evidence) in the opposite direction. Due to confinement effect of water, some of the melt debris immediately re-solidifies and adheres to the ablated sides as well. The similar patterns follow when the laser scan starts machining at the second edge of channel. In this way, the central region of channel accumulates more number of deposited debris. For this central region, the focus of laser spot does not remain at the surface rather the focus goes inside the central peaked region. In similar fashion, the same material ejection phenomenon repeats for each forthcoming scanning pass and thus the laser beam focus goes deeper and deeper for this central location of channel. Such out-focusing causes the material under laser irradiations just to heat up instead of melting or partial melting. The re-deposited melt debris loosely adheres at the middle region; thus, upon heating and partial melting, these deposited debris re-melted and flushed away under high-pressure water plume. On the other end, melting of base metal at this middle region does not happen due to the insufficient heat for melting. Insufficient heat for the base metal to melt could be the result of many factors including drop of laser intensity due to water, water light absorption, melt debris deposited above surface, and disturbed beam focus. Consequently, the channel gets divided into two V-shaped sub-channels having peak at middle.

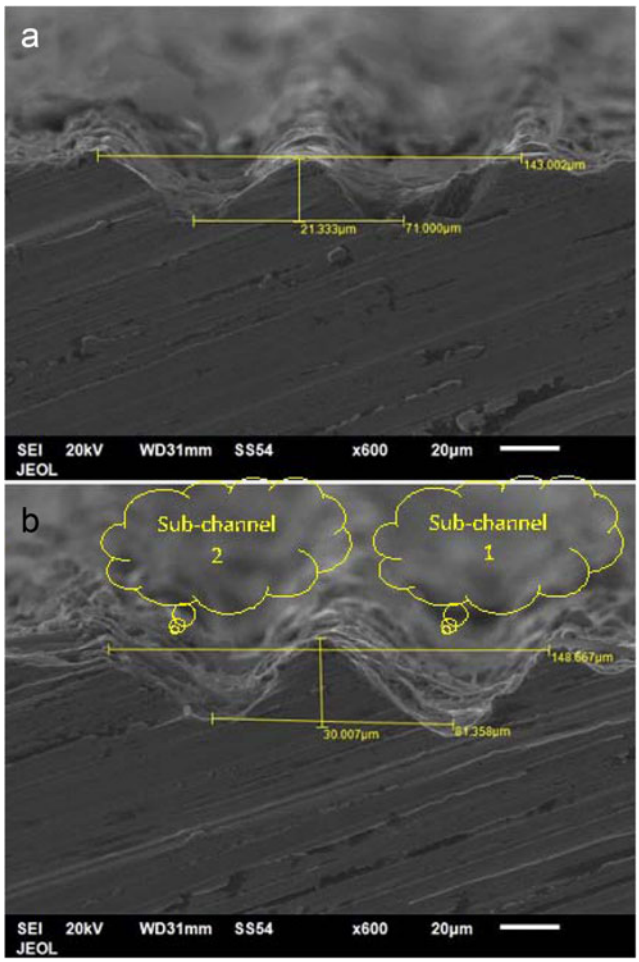

Fig. 4 Micro-channels fabricated under water at **a** I=28.32 W, f=35 kHz, v=350 mm/s, t=1 mm and **b** I=28.92 W, f=40 kHz, v=400 mm/s, t=1 mm

4.2 Micro-channels under high scan speeds

The previous discussion shows that low scan speeds generate micro-channels with coarse profile. Therefore, high scan speeds (ranging 70–400 mm/s) were decided to employ. Hence, in this set of experimental runs, the micro-channels of same cross-sectional size of 100 × 100 μm were machined by varying the ranges of all the three predictors. These settings include laser power of 27.72–28.92 W, pulse repetition rate of 30–40 kHz, scan speed of 70–400 mm/s (a successive increment of 25 mm/s), and the average water film thickness of 1 mm. The selection of these ranges was the result of pilot experimental runs and the procedural advices of laser system used that provides the combinations of repetition rate and scan speed against each level of laser power. However, the levels of scan speeds were slightly violated from the laser system's guidelines. The selected images of the resulted machined geometries are presented in Figs. 4 and 5. Again, two sub-channels were produced under high scan speeds as were in the case of low scan speeds. The geometrical aspects were more promising in this case of high scan speeds with varying laser power and pulse repetition rate. These sub-channels were

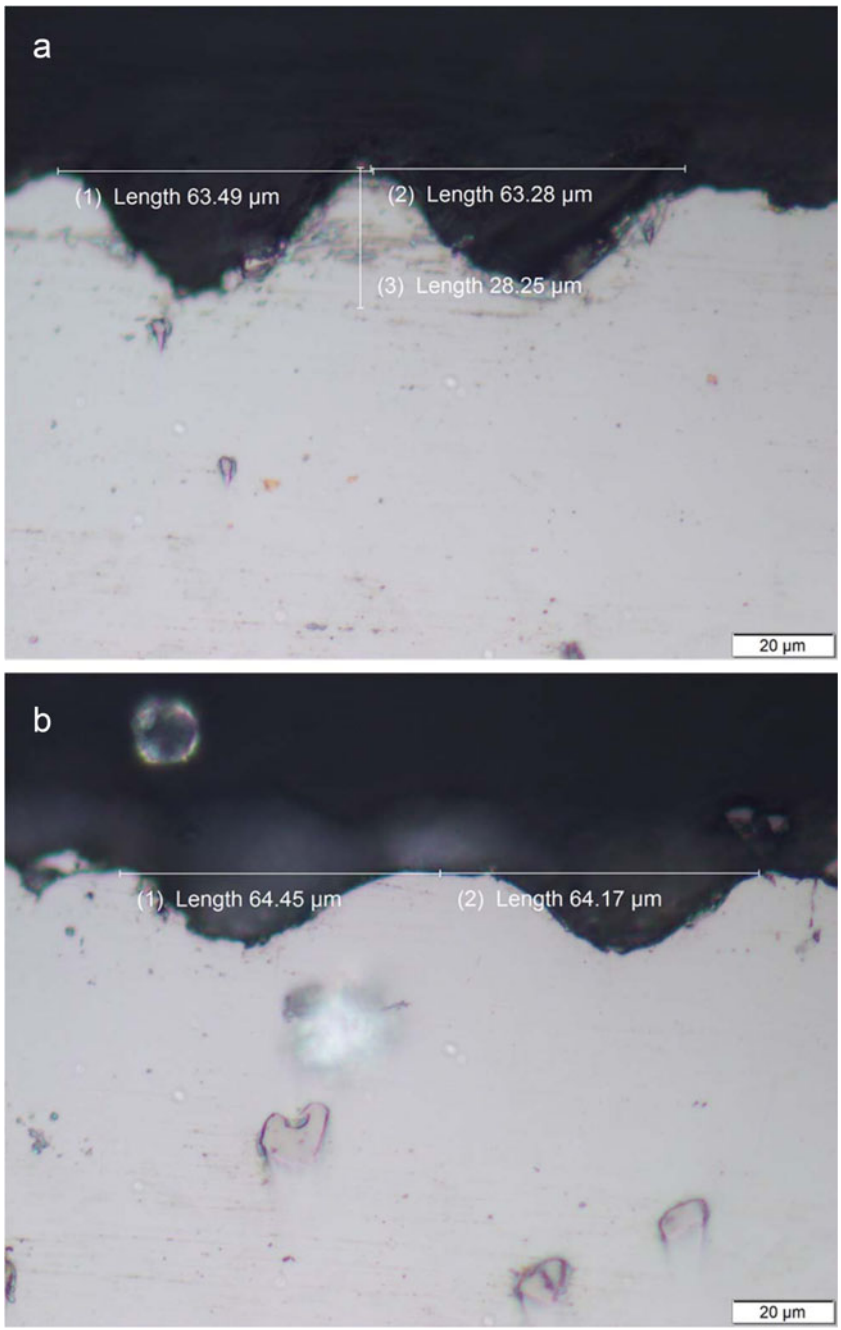

Fig. 5 **a**, **b** Microscopic images of single micro-channel divided into two micro-channels

more clear and discernable as pointed out by cloud callouts in Fig. 4b. The main governing phenomenon of these fine channels' geometries is the appropriate laser interaction time with the machining surface due to high scan speed. The amount of melt material per laser scan was sufficient enough that can be easily flushed away by water plume. As there was no excess of material removal per scan, therefore, the depth of sub-channel in this case was not similar to the previous case of low scan speeds. Due to this low depth of channel, the melt debris have to travel less upward vertical distance and ejects away easily by the plume. Thus, the resulted micro-channels were clean and more uniform in shape. The significant amount of re-deposition of debris was observed only at the edges of channel. The periphery of water plume terminates at the edges of the channel and flushing performance of the water plume reduces at its peripheral boundary. Hence, some of the debris could not properly flush away and stayed out at the edges resulting into a burr at channel's edges.

4.3 Analysis of parametric effects

The study is conducted to evaluate the effect of three laser-based parameters named laser power, pulse repetition rate, and scan speed against three process performance-based responses named width, depth, and taper angle. The main effects of laser parameters on the set responses are furnished in the following subsections. This discussion will mainly revolve around the content of Fig. 6.

4.3.1 Effect of scan speed

The influence of scan speed on process throughput is categorized into two regions (illustrated in Fig. 6a). The region enclosed in circular callout is the low scan speed region (10–60 mm/s), while the remaining area is associated with high scan speeds (70–400 mm/s). There is a symmetrical zigzag-shaped variation in channel's width (*W*) of average size of 80 μm against all the low scan speeds except for 45 mm/s

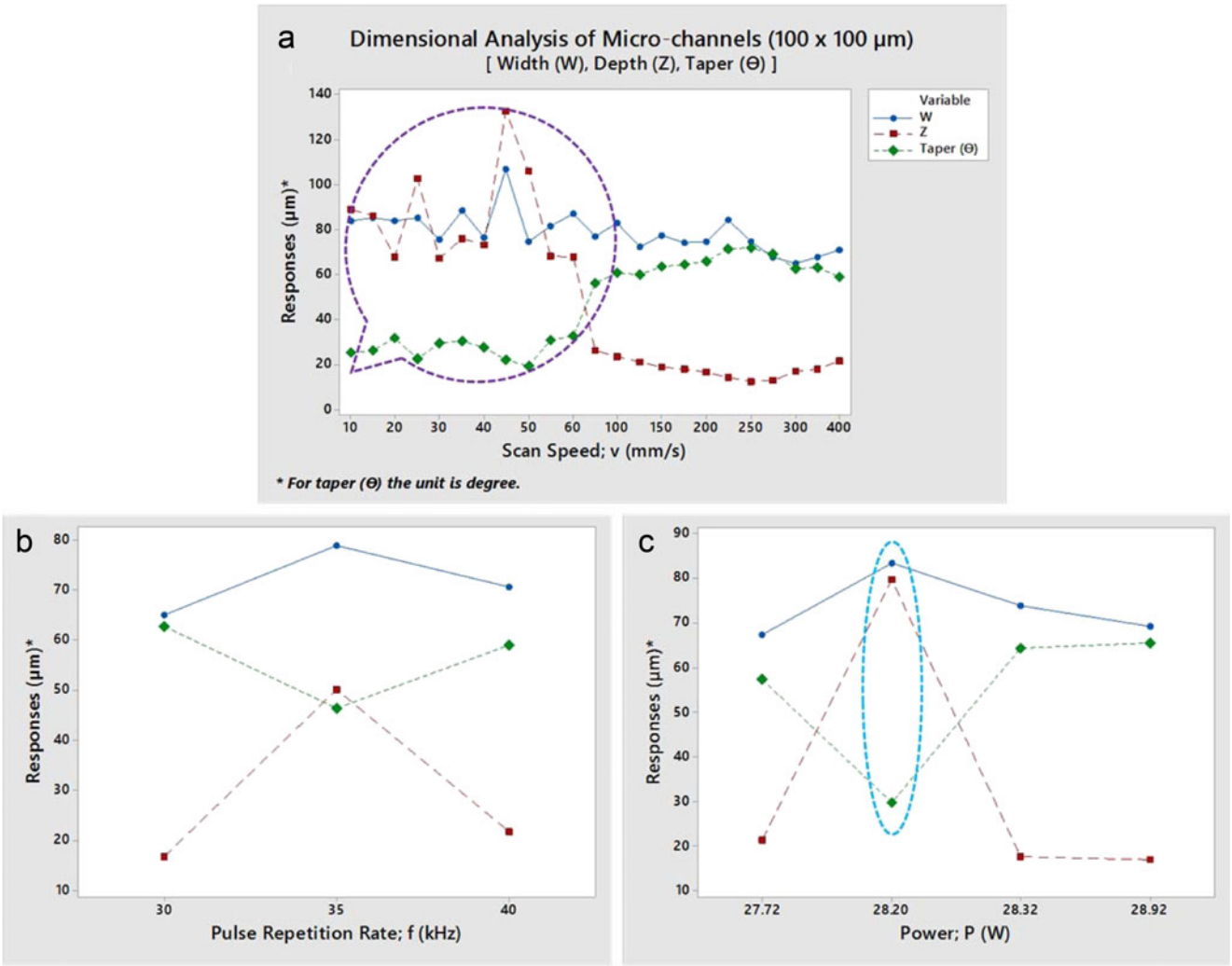

Fig. 6 Dimensional analysis of micro-channels of size 100×100 μm: **a** impact of scan speed, **b** impact of pulse repetition rate, and **c** impact of laser power

where the width is 100 μm. On the other hand, the depth (*Z*) of channel follows a huge variation from 60 to 135 μm under these low scan speeds. The taper (θ) of channel's side walls has no odd point and remains at an average value of 30°. Coming to the right side of Fig. 6a, the response of high speeds in term of channel width (*W*) is more consistent than that of low speeds. There is a slight decrease in channel width (*W*) reaching at an average of 60 μm when the scan speed lies in high ranges, especially from 200 to 400 mm/s. The depth (*Z*) and taper (θ) follows uniform relations when the scan speed is within 70–400 mm/s. Under this high speed regime, an average depth of channel is 25 μm and taper of 50°. It can also be observed that the taper and depth of channel are reciprocal of each other. High values of depth allow the taper to shrink, whereas low values of depth relatively expand the taper (in both the case of low and high scan speeds).

4.3.2 Effect of pulse repetition rate

The mean effect of pulse repetition rate is depicted in Fig. 6b. Three levels of repetition rate (30, 35, and 40 kHz) are employed with uniform increment of 5 kHz. It can be perceived that all the three levels give an average channel width (*W*) of 65–80 μm. The minimum taper (θ) of approximately 45° can be achieved using pulse repetition rate of 35 kHz. The depth (*Z*) of average size 20 μm is achievable using repetition rate of 30 and 40 kHz, whereas to realize the maximum depth of 50 μm, a repetition rate of 35 kHz is more favorable. Instead, the repetition rate of 35 kHz is more suitable to obtain maximum width and depth and minimum taper of channel during machining of Inconel 718 under water environment of static mode.

4.3.3 Effect of laser power

The effect of laser power on each of three responses is demonstrated in Fig. 6c. The elliptical callout mentioned here is the outlier observation of all the responses over laser power of 28.2 W. This region is basically the result of low scan speeds employed with constant laser power of 28.2 W that correspondingly yields higher values of each response. If we ignore this elliptical region for a while, then it can be clearly seen that the laser power influences each of responses to follow a uniform pattern. This is the effect of laser energy attenuation in fluidic atmosphere where significant amount of energy absorption by fluid film always occurs. There is no significant change in attenuation rate of energy levels when the laser power levels are close to each other. As in this current study, the power levels are 27.72, 28.32, and 28.92 with just an increment of ~0.5 W; therefore, the amount of energy which reaches to the substrate surface remains closer to each other at these closely defined levels. That is why all of the responses show a very little variation even when the laser power increases from 27.72 to 28.92 W. Hence, the important parameter that controls the set responses is the scan speed. It is very clear that inside the elliptical region (where the scan speeds are very low; 10–60 mm/s) the power is 28.2 W, but the responses reached at unexpected dimensions. When the scan speed is at high value (hundreds of mm/s) and laser power levels varying very close to each other (very few of *W*, e.g., 0.5 W), the laser power does not majorly influence the channel's geometries.

5 Conclusions

The investigational outcomes discussed above have demonstrated that the laser beam machining in the presence of static water film above work sample is a potential candidate of machining micro-channels in nickel-based superalloy. The channel's geometries and appearance can be controlled by the optimized process parameters. It can be concluded that the underwater LBM with static mode of water can generate two sub-channels instead of one micro-channel. It can also be said that laser beam machining under water immersion is twofold productive than dry LBM as it can allow to fabricate two channels in place of one. The governing phenomenon behind the fabrication of sub-channels is the use of re-deposition of melt debris due to the presence of static water film above substrate surface and the disturbance of beam focus. Among the laser parameters investigated in this study, laser scan speed affects the geometrical characteristics of micro-channels more severely than the other parameters. High scan speeds (100–400 mm/s) are more appropriate. Laser power (ranging within 27.72–28.92 W) does not impart any significant impact on the set responses due to the attenuation of laser energy occurred when laser beam passes through water. However, the repetition rate of 35 kHz is more suitable to obtain maximum width and depth with minimum taper of channel's side walls.

Acknowledgments The project was financially supported by King Saud University, Vice Deanship of Research Chairs.

References

1. Kazakevich PV, Simakin AV, Voronov VV, Shafeev GA (2006) Laser induced synthesis of nanoparticles in liquids. Appl Surf Sci 252(13):4373–4380
2. Tangwarodomnukun V, Wang J, Huang CZ, Zhu HT (2012) An investigation of hybrid laser–waterjet ablation of silicon substrates. Int J Mach Tools Manuf 56:39–49
3. Mahdieh MH, Nikbakht M, Eghlimi Moghadam Z, Sobhani M (2010) Crater geometry characterization of Al targets irradiated by single pulse and pulse trains of Nd:YAG laser in ambient air and water. Appl Surf Sci 256(6):1778–1783
4. Morita N, Ishida S, Fujimori Y, Ishikawa K (1988) Pulsed laser processing of ceramics in water. Appl Phys Lett 52:1965
5. Stephan Roth MG (2000) Novel technique for high-quality microstructuring with excimer lasers

6. Zhu S, Lu YF, Hong MH, Chen XY (2001) Laser ablation of solid substrates in water and ambient air. J Appl Phys 89(4):2400–2403
7. Peyre P, Berthe L, Scherpereel X, Fabbro R (1998) Laser-shock processing of aluminium-coated 55C1 steel in water-confinement regime, characterization and application to high-cycle fatigue behaviour. J Mater Sci 33(6):1421–1429
8. Dolgaev SI, Lyalin AA, Shafeev GA, Voronov S (1996) Fast etching and metallization of SiC ceramics with copper-vapor-laser radiation. Appl Phys A 63(1):75–79
9. Voronov VV, Dolgaev SI, Lyalin AA, Shafeev GA (1996) Laser-assisted etching of the surface of polycrystalline silicon carbide by copper-vapour laser radiation. Quantum Electron 26(7):621
10. Patel DN, Singh RP, Thareja RK (2014) Craters and nanostructures with laser ablation of metal/metal alloy in air and liquid. Appl Surf Sci 288:550–557
11. Ohara MNOJ (1997) High aspect ratio etching by infrared laser induced micro bubbles. 175–179
12. Choo KL, Ogawa Y, Kanbargi G, Otra V, Raff LM, Komanduri R (2004) Micromachining of silicon by short-pulse laser ablation in air and under water. Mater Sci Eng A 372(1–2):145–162
13. Geiger M, Becker W, Rebhan T, Hutfless J, Lutz N (1996) Increase of efficiency for the XeCl excimer laser ablation of ceramics. Appl Surf Sci 96–98:309–315
14. Kruusing A, Leppävuori S, Uusimäki A, Petrêtis B, Makarova O (1999) Micromachining of magnetic materials. Sensors Actuators A Phys 74(1–3):45–51
15. Li Y, Itoh K, Watanabe W, Yamada K, Kuroda D, Nishii J, Jiang Y (2001) Three-dimensional hole drilling of silica glass from the rear surface with femtosecond laser pulses. Opt Lett 26(23):1912–1914
16. Tangwarodomnukun V, Likhitangsuwat P, Tevinpibanphan O, Dumkum C (2015) Laser ablation of titanium alloy under a thin and flowing water layer. Int J Mach Tools Manuf 89:14–28
17. Dowding CF, Lawrence J (2009) Impact of open de-ionized water thin film laminar immersion on the liquid-immersed ablation threshold and ablation rate of features machined by KrF excimer laser ablation of bisphenol A polycarbonate. Opt Lasers Eng 47(11):1169–1176
18. Daminelli G, Krüger J, Kautek W (2004) Femtosecond laser interaction with silicon under water confinement. Thin Solid Films 467(1–2):334–341
19. Acherjee B, Prakash S, Kuar AS, Mitra S (2014) Grey relational analysis based optimization of underwater Nd:YAG laser microchanneling on PMMA. Procedia Eng 97:1406–1415
20. Kang HW, Lee H, Welch AJ (2008) Laser ablation in a liquid-confined environment using a nanosecond laser pulse. J Appl Phys 103(8):083101
21. Klocke F, Welling D, Klink A, Veselovac D, Nöthe T, Perez R (2014) Evaluation of advanced wire-EDM capabilities for the manufacture of fir tree slots in Inconel 718. Procedia CIRP 14:430–435
22. Manohar M, Selvaraj T, Sivakumar D, Gopinath S, George KM (2014) Experimental study to assess the effect of electrode bottom profiles while machining Inconel 718 through EDM process. Procedia Mater Sci 6:92–104
23. Escobar-Palafox GA, Gault RS, Ridgway K (2012) Characterisation of abrasive water-jet process for pocket milling in Inconel 718. Procedia CIRP 1:404–408
24. Klocke F, Zeis M, Klink A, Veselovac D (2013) Technological and economical comparison of roughing strategies via milling, sinking-EDM, wire-EDM and ECM for titanium- and nickel-based blisks. CIRP J Manuf Sci Technol 6(3):198–203
25. Rajurkar KP, Sundaram MM, Malshe AP (2013) Review of electrochemical and electrodischarge machining. Procedia CIRP 6:13–26
26. Venkatesan K, Ramanujam R, Kuppan P (2014) Analysis of cutting forces and temperature in laser assisted machining of Inconel 718 using Taguchi method. Procedia Eng 97:1637–1646
27. Attia H, Tavakoli S, Vargas R, Thomson V (2010) Laser-assisted high-speed finish turning of superalloy Inconel 718 under dry conditions. CIRP Ann Manuf Technol 59(1):83–88
28. Venkatesan K, Ramanujam R, Kuppan P (2014) Laser assisted machining of difficult to cut materials: research opportunities and future directions—a comprehensive review. Procedia Eng 97:1626–1636
29. Brehl DE, Dow TA (2008) Review of vibration-assisted machining. Precis Eng 32(3):153–172
30. Leshock CE, Kim J-N, Shin YC (2001) Plasma enhanced machining of Inconel 718: modeling of workpiece temperature with plasma heating and experimental results. Int J Mach Tools Manuf 41(6):877–897
31. Abdul Aleem BJ, Hashmi MSJ, Yilbas BS (2011) Laser controlled melting of pre-prepared inconel 718 alloy surface. Opt Lasers Eng 49(11):1314–1319
32. Yilbas BS, Akhtar SS, Karatas C (2010) Laser surface treatment of Inconel 718 alloy: thermal stress analysis. Opt Lasers Eng 48(7–8):740–749
33. Mori Seiki D. DMG Middle East FZE, Jebel Ali Free Zone, JAFZA Towers, Lob 18, Office 2403, P.O. Box, Dubai, U.A.E." [Online]. Available: http://www.dmgmoriseiki.com/
34. Teixidor D, Ferrer I, Ciurana J, Özel T (2013) Optimization of process parameters for pulsed laser milling of micro-channels on AISI H13 tool steel. Robot Comput Integr Manuf 29(1):209–218
35. Instruments H. Hanna Instruments, Rhode Island, 584 Park East Drive Woonsocket, RI 02895. [Online]. Available: http://www.hannainst.com/usa/
36. Metals M. Magellan Industrial Trading Company, Inc. (dba Magellan Metals), 227 Wilson Avenue. South Norwalk, CT 06854 U.S.A. [Online]. Available: http://www.magellanmetals.com/
37. Weber R, Hafner M, Michalowski A, Graf T (2011) Minimum damage in CFRP laser processing. Phys Procedia 12(Part B):302–307
38. Perry TL, Werschmoeller D, Li X, Pfefferkorn FE, Duffie NA (2009) Pulsed laser polishing of micro-milled Ti6Al4V samples. J Manuf Process 11(2):74–81
39. Lee SW, Shin HS, Chu CN (2013) Fabrication of micro-pin array with high aspect ratio on stainless steel using nanosecond laser beam machining. Appl Surf Sci 264:653–663
40. Dai Y-T, Xu G, Tong X-L (2012) Deep UV laser etching of GaN epilayers grown on sapphire substrate. J Mater Process Technol 212(2):492–496
41. Yan Y, Li L, Sezer K, Wang W, Whitehead D, Ji L, Bao Y, Jiang Y (2011) CO2 laser underwater machining of deep cavities in alumina. J Eur Ceram Soc 31(15):2793–2807
42. Cicală E, Soveja A, Sallamand P, Grevey D, Jouvard JM (2008) The application of the random balance method in laser machining of metals. J Mater Process Technol 196(1–3):393–401
43. Nieto D, Delgado T, Flores-Arias MT (2014) Fabrication of microchannels on soda-lime glass substrates with a Nd:YVO4 laser. Opt Lasers Eng 63:11–18
44. Al-Mamun SA, Nakajima R, Ishigaki T (2012) Effect of liquid level and laser power on the formation of spherical alumina nanoparticles by nanosecond laser ablation of alumina target. Thin Solid Films 523:46–51
45. Long Y, Shi T, Xiong L (2010) Excimer laser electrochemical etching n-Si in the KOH solution. Opt Lasers Eng 48(5):570–574
46. Dowding C, Lawrence J (2010) Effects of closed immersion filtered water flow velocity on the ablation threshold of bisphenol A polycarbonate during excimer laser machining. Appl Surf Sci 256(12):3705–3713
47. Mullick S, Madhukar YK, Roy S, Kumar S, Shukla DK, Nath AK (2013) Development and parametric study of a water-jet assisted underwater laser cutting process. Int J Mach Tools Manuf 68:48–55
48. E. Machine tool manufacturer. 24/2 Nanded, Taluka: Haveli District:Pune, Maharashtra, INDIA 411041. Electronica. [Online]. Available: http://www.electronicagroup.com/